

CT imaging features of COVID-19 pneumonia: initial experience from Turkey

Akın Çinkooğlu 
Cenk Hepdurgun 
Selen Bayraktaroğlu 
Naim Ceylan 
Recep Savaş 

PURPOSE

We aimed to demonstrate the computed tomography (CT) findings observed at the initial presentation of coronavirus disease 2019 (COVID-19) pneumonia and reveal the most frequent infiltration and distribution patterns of the disease.

METHODS

A total of 185 patients (87 men, 98 women; mean age, 48.7 years), who underwent RT-PCR sampling and high-resolution CT examination at our hospital between March 15, 2020, and April 15, 2020, and got a definitive diagnosis of COVID-19 disease via initial or follow-up RT-PCR test, were included in the study. We comprehensively analyzed the most common and relatively rare CT imaging features (e.g., distribution pattern, density of the lesions, additional CT signs) in patients diagnosed with COVID-19 pneumonia.

RESULTS

Thirty-eight patients (20.6%) had no evidence of pneumonia on their initial high-resolution CT images. Among 147 patients (79.4%) who had parenchymal infiltration consistent with pneumonia, 10 (6.8%) had a negative baseline RT-PCR test, and positivity was detected as a result of repeated tests. Most of the patients had multifocal (89.1%) and bilateral (86.4%) lesions. The most common location, right lower lobe, was affected in 87.8% of the patients. Lesions were distributed predominantly at peripheral (87.1%) and posterior (46.3%) areas of lung parenchyma. Most of the patients had pure ground glass opacity (GGO) (82.3%) followed by GGO with consolidation (32.7%) and crazy paving pattern (21.8%). Pure consolidation, solid nodules, halo sign, reverse halo sign, vascular enlargement, subpleural line, air-bronchogram, and bronchiectasis were the other findings observed in at least 15% of the cases. Halo sign, acinar nodules, air-bubble sign, pleural thickening and effusion, mediastinal and/or hilar lymphadenopathy were seen rarely (2%–12.9%). Pericardial effusion, pneumothorax, cavitation, and tree-in-bud pattern were not detected in our study group.

CONCLUSION

Multifocal and bilateral GGO infiltration predominantly distributed in peripheral, posterior, and lower lung areas was the most common infiltration pattern.

The novel coronavirus named “severe acute respiratory syndrome coronavirus-2” (SARS-CoV-2) was first reported in Wuhan, China in December 2019 and spread all around the world (1). World Health Organization (WHO) named the disease caused by SARS-CoV-2 as coronavirus disease 2019 (COVID-19) and declared this global outbreak as a pandemic (2). As of April 23, 2020, in Turkey, there are 101 790 confirmed cases, with 2491 cases of mortality (3).

Early diagnosis and isolation are important to control the spread due to easy transmission from person to person through close contact, droplets, and aerosols (4). Confirmation of the diagnosis is made by the real-time reverse transcription-polymerase chain reaction (RT-PCR) test as the reference standard, and in a meta-analysis, the pooled sensitivity of RT-PCR was reported to be 89% (5). Computed tomography (CT) is a simple and readily available imaging modality that can quickly detect lung lesions at the early stage with a high sensitivity rate, especially in cases with high clinical suspicion and negative RT-PCR test results at initial

Department of Radiology (A.Ç. ✉ acinko@gmail.com), Ege University Faculty of Medicine, Izmir, Turkey.

Received 03 May 2020; revision requested 22 May 2020; last revision received 24 May 2020; accepted 28 May 2020.

Published online 17 June 2020.

DOI 10.5152/dir.2020.20307

You may cite this article as: Çinkooğlu A, Hepdurgun C, Bayraktaroğlu S, Ceylan N, Savaş R. CT imaging features of COVID-19 pneumonia: initial experience from Turkey. *Diagn Interv Radiol* 2020; 26:308–314.

presentation (6–8). By now, a diverse range of CT findings that can guide radiologists in the diagnosis of the disease have been analyzed and some of them were defined as more typical for COVID-19 pneumonia (9).

In our study, we aimed to demonstrate the CT findings observed at the initial presentation of COVID-19 pneumonia and reveal the most frequent infiltration and distribution patterns of the disease.

Methods

Patients

This study was approved by the medical ethics committee of our institution (Approval Number: 20-4.2T/19) and the Republic of Turkey Ministry of Health, COVID-19 Scientific Research Committee. All patients gave informed consent. We retrospectively reviewed 206 patients who underwent RT-PCR sampling and CT examination in our hospital between March 15, 2020, and April 15, 2020, and got a definitive diagnosis of COVID-19 disease by initial or follow-up positive RT-PCR test result. The inclusion criteria were as follows: 1) initial RT-PCR test performed on admission day; 2) chest CT examination done within 24 hours after RT-PCR testing; 3) images taken with high-resolution CT protocol. Being under the age of 18 was determined as the exclusion criterion. A total of 185 patients (87 men and 98 women; age range, 18–95 years; mean age, 48.7 years) who met the above criteria were included in our study group (Fig. 1).

CT imaging and evaluation

Images were taken via a 160-slice CT scanner (Aquilion Prime, Toshiba Medical Systems). The axial images were acquired craniocaudally at shallow inspiration and included the body part from the thoracic inlet to the diaphragm. Images were taken at high-resolution CT protocol with 120 kVp, 100–200 mA, 80×0.5 mm collimation

Main points

- A diverse group of chest CT findings can be seen in COVID-19 pneumonia.
- Pure ground glass opacities were present in most of our cases.
- Lung involvement tended to be bilateral with multifocal lesions distributed mainly at peripheral areas of the lower lobes.
- Chest CT has a complementary role in the diagnosis of the disease.

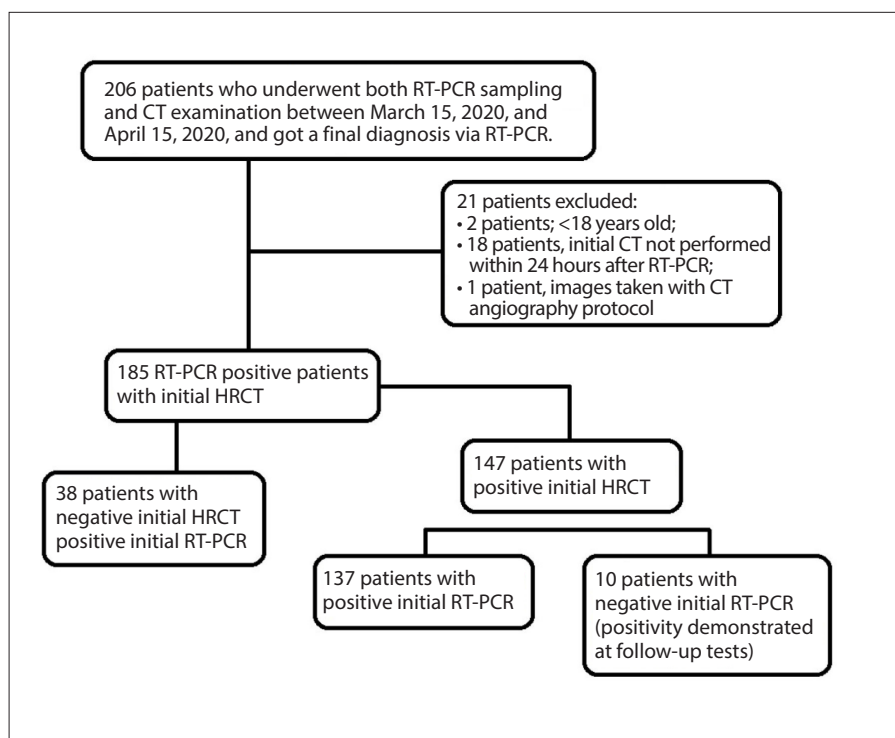


Figure 1. Flowchart of patient selection. RT-PCR, reverse transcription-polymerase chain reaction; CT, computed tomography; HRCT, high-resolution CT.

and reconstructed at 0.5 mm slice thickness with a sharp reconstruction kernel.

CT images were evaluated independently by two radiologists with 6 and 16 years of experience in thoracic imaging. Final decisions were reached by consensus. For the cases causing disagreement between the two primary radiologists, a third thoracic radiologist with 25 years of experience made a final decision. Following CT characteristics were evaluated: 1) location and distribution of the lesions, i.e., focality, laterality, lobar, transverse, craniocaudal, anteroposterior, and peribronchovascular distributions; 2) density of the lesions, i.e., pure ground glass opacity (GGO), GGO with consolidation, crazy paving pattern, pure consolidation, solid nodules, halo sign, reverse halo sign, acinar nodules, cavitation, tree in bud; 3) other CT features, i.e., air bronchogram, air bubble sign, subpleural line, parenchymal distortion, vascular enlargement, bronchiectasis, pleural thickening, pleural effusion, mediastinal-hilar lymphadenopathy, pericardial effusion, pneumothorax.

Statistical analysis

Continuous data were expressed as mean and standard deviation, while categorical data were expressed as counts (n) and percentages (%). All statistical analyses

were performed with SPSS software (version 25.0, IBM).

Results

We evaluated CT images of RT-PCR test positive 185 patients with the final diagnosis of COVID-19 disease. Of these patients, 147 (79.4%) had parenchymal infiltration consistent with pneumonia. Ten patients (6.8%) had a negative initial RT-PCR test result; however, infiltration was present on CT. The mean interval time between the initial negative and follow-up positive RT-PCR results was 1.7 ± 0.8 days (Table 1).

A diverse range of CT findings of 147 COVID-19 pneumonia patients (70 men and 77 women; age range, 19–85 years; mean age, 51 years) were analyzed in our study. We evaluated the location, distribution, and opacification pattern of the infiltration. Additional CT findings and signs reported in the literature were also evaluated. Most of the patients had multifocal lesions (89.1%). Bilateral involvement was identified in 127 cases (86.4%). Lower lobes were the most affected lobes, and only 8 patients (5.4%) had both lower lobes preserved. Compared to the left lower lobe (85.7%), there was a slight tendency for right lower lobe involvement (87.8%). Two or more lobes were affected in 131 cases (89.1%), and 54 cases (70.9%)

Table 1. Patient characteristics		
RT-PCR positive patients (n=185)	Pneumonia (+) (n=147)	Pneumonia (-) (n=38)
Age (years), mean±SD	51.0±15.8	39.9±14.0
Gender	70 men, 77 women	17 men, 21 women
RT-PCR positivity at first test, n (%)	137 (93.2)	38 (100)
RT-PCR positivity at second test, n (%)	8 (5.4)	-
RT-PCR positivity at third test, n (%)	2 (1.4)	-
Interval to RT-PCR positivity* (days), mean±SD	1.7±0.8	-

RT-PCR, reverse transcription - polymerase chain reaction.
*The time interval between the initial negative and follow-up positive test.

Table 2. CT imaging findings of COVID-19 pneumonia (n=147)					
Location / Distribution	n	%	Density	n	%
Focality			Pure GGO	121	82.3
Unifocal	16	10.9	GGO with consolidation	48	32.7
Multifocal	131	89.1	Crazy paving pattern	32	21.8
Laterality			Pure consolidation	22	15.0
Unilateral	20	13.6	Solid nodules	27	18.4
Bilateral	127	86.4	Other CT findings		
Lobar distribution			Halo sign	15	10.2
Right lower lobe	129	87.8	Reverse halo sign	22	15.0
Right middle lobe	105	71.4	Air-bronchogram	34	23.1
Right upper lobe	114	77.6	Air-bubble sign	15	10.2
Left lower lobe	126	85.7	Acinar nodules	15	10.2
Left upper lobe	119	81.0	Transverse distribution		
Transverse distribution			Subpleural line	41	27.9
Central predominant	3	2.0	Vascular enlargement	50	34.0
Peripheral predominant	128	87.1	Bronchiectasis	28	19.0
No predominancy	16	10.9	Pleural thickening	19	12.9
Craniocaudal distribution			Pleural effusion	3	2.0
Upper lung predominant	14	9.5	Mediastinal and/or hilar LAP	18	12.2
Lower lung predominant	76	51.7	Anteroposterior distribution		
No predominancy	57	38.8	Cavitation		
Anteroposterior distribution			Tree-in-bud		
Anterior lung predominant	13	8.8	Pericardial effusion		
Posterior lung predominant	68	46.3	Pneumothorax		
No predominancy	66	44.9	Other location / distribution features		
Other location / distribution features					
Peribronchovascular distribution	35	23.8			
Peripheral lesions with long axis parallel to pleura	61	41.5			

CT, computed tomography; COVID-19, coronavirus disease 2019; GGO, ground glass opacity; LAP, lymphadenopathy.



Figure 2. HRCT image of a 59-year-old female COVID-19 patient presenting with fever and dry cough for 3 days. Bilateral GGOs distributed predominantly at peripheral and posterior areas of lower lobes (arrows). This pattern was defined as typical for COVID-19 pneumonia and was present with a high incidence among our cases.

these location and distribution characteristics in our study group, a solitary lesion located in the upper lobe was a rare finding, seen only in 4 of 147 cases.

Of 147 patients with abnormal CT, the vast majority (97.3%) had at least one lesion with GGO component. Among these, pure GGO (patchy and/or nodular) was the most common pattern (82.3%), followed by GGO with consolidation (32.7%) and crazy paving pattern (21.8%). Pure GGO was the only finding in 60 cases (40.8%). Pure consolidation was relatively rare and observed in 22 cases (15%). Although these infiltrations had different shape and margin features, peripheral infiltrations with the long axis running parallel to pleura were observed in a considerable amount of the cases (41.5%). Multifocal solid nodules were seen on the CT images of 27 patients (18.4%), and nodules with peripheral GGO halo (halo sign) were present in 15 of them. Another CT finding, "reverse halo sign", described as a central rounded GGO surrounded by a ring-like consolidation (10), was observed on 22 CT scans (15%). Additional CT findings accompanying all these different infiltration patterns were also present. Of these, the most common finding was vascular enlargement defined as the dilatation of pulmonary vessels around and within the lesions (9) and was seen on 50 CT scans (34%). A thin curvilinear opacity parallel to the pleural surface with a 1–3 mm thickness named "subpleural line" (10) was another frequent finding (27.9%) followed by air-bronchogram (23.1%), bronchiectasis (19%), parenchymal distortion (17.7%). As a relatively rare finding, we observed small air-containing spaces in some of the infiltrations, named "air-bubble sign" (10.2%) (9).

had diffuse infiltration involving all of the lung lobes. Lesions were distributed mainly at peripheral (87.1%) and posterior (46.3%)

areas of lung parenchyma (Fig. 2). Peribronchovascular distribution was a rare finding observed in 35 cases (23.8%). Considering

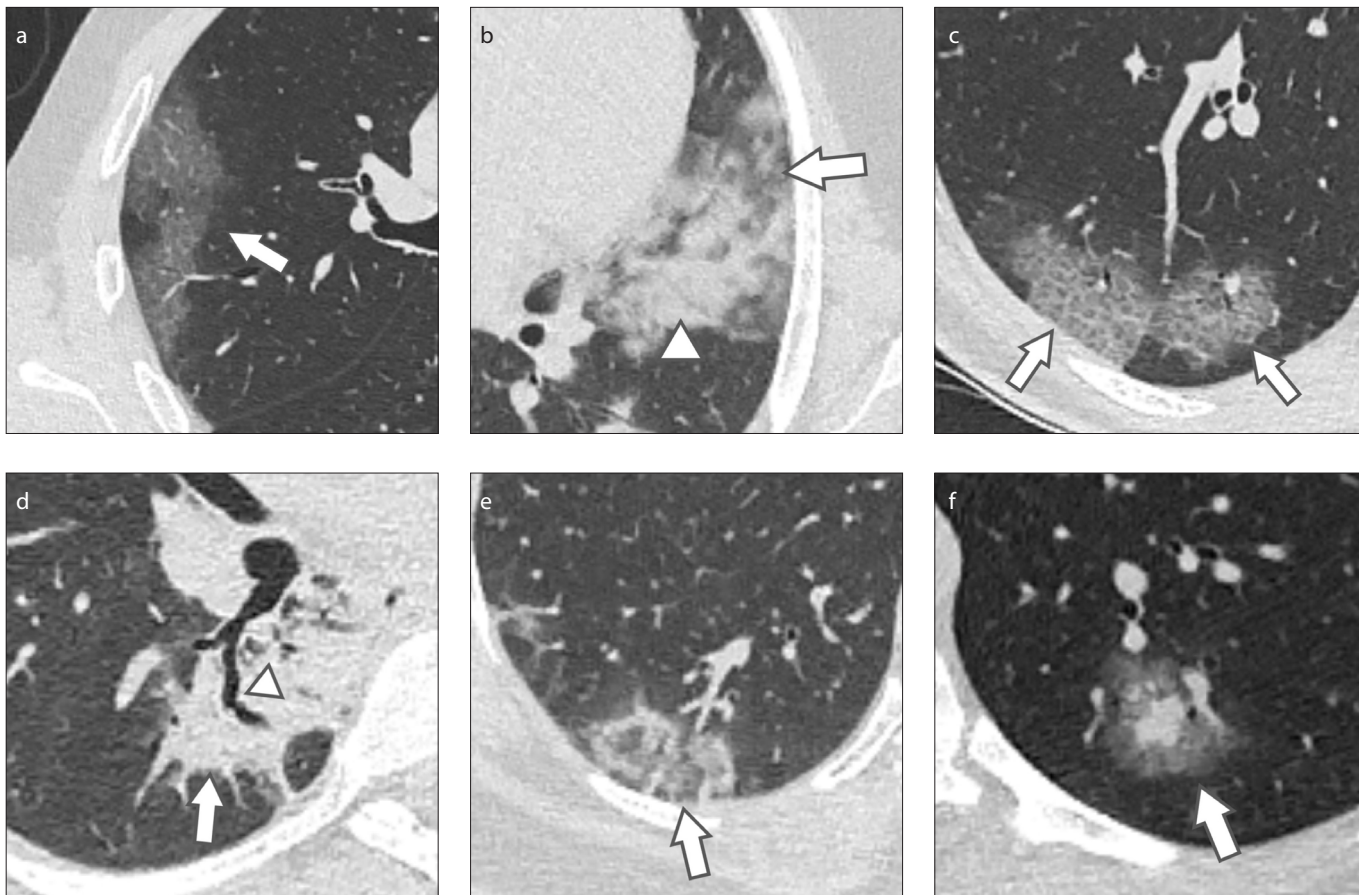


Figure 3. a–f. HRCT images demonstrate examples of different infiltration patterns of COVID-19 pneumonia: (a), peripheral pure GGOs (arrow); (b), GGO (arrow) with consolidation (arrowhead); (c), GGO with interlobular septal, intralobular interstitial thickening defined as “crazy-paving pattern” (arrows); (d), pure consolidation (arrow) with “air-bronchogram” (arrowhead); (e), “reverse halo sign” described as a central rounded GGO surrounded by a ring-like consolidation (arrow); and (f), solid nodule with peripheral GGO “halo sign” (arrow).

In our study group, no tree-in-bud pattern or cavitation was observed. As for extraparenchymal findings, pleural thickening was more common (12.9%) than pleural effusion (2%). Mediastinal and/or hilar lymphadenopathy were seen on 18 CT scans (12.2%). Pneumothorax and pericardial effusion were not detected in our cases. Table 2 summarizes the CT imaging findings mentioned above. Examples of CT findings are shown in Figs. 3 and 4.

Discussion

We comprehensively analyzed the chest CT characteristics in patients diagnosed with COVID-19 pneumonia. This is the initial report of radiologic findings detected in our country, Turkey. A total of 185 patients with a final diagnosis of COVID-19 infection, whose initial RT-PCR test was performed on the day of admission to our hospital and whose high-resolution CT images were taken within 24 hours after RT-PCR testing, were evaluated. Lung infiltration consistent

with pneumonia was seen on CT images of 147 patients. Ten of them (6.8%) had a negative baseline RT-PCR test result, and positivity was detected as a result of repeated tests. Therefore, CT imaging enabled early diagnosis in this group of patients. Ai et al. (6) mentioned the complementary role of CT in patients with false-negative RT-PCR test results. Using RT-PCR as the reference, they reported the sensitivity of chest CT imaging as 97%. Failure in sample collection, transportation, or kit performance can be listed as factors limiting the accuracy of RT-PCR testing (11). In addition, interpretation of CT images can be easily done within minutes after the scan, whereas getting RT-PCR test results generally takes longer. Given the need for early diagnosis and isolation, this can be seen as the advantage of CT imaging. However, in addition to the high sensitivity of CT, low specificity should also be taken into consideration. Kim et al. (5) mentioned the high sensitivity, but low specificity of chest CT in their meta-analy-

sis, in which the positive predictive value of RT-PCR was reported to be ten times higher than that of CT in low-prevalence countries. Also, it should be kept in mind that a chest CT may be normal in the early period of the disease. Bernheim et al. (12), in their study with 121 confirmed COVID-19 cases, reported that 56% of patients imaged early, at 0–2 days after symptom onset, had a normal CT with complete absence of GGOs and consolidation. Of our patients, 20.6% (38/185) had no parenchymal infiltration consistent with pneumonia, whereas all had an initial positive RT-PCR test.

In our study, the most common and relatively rare CT findings of the disease were evaluated based on the location of the lesions, distribution, and opacification patterns. Pure GGO was the most common imaging finding (82.3%). Multifocal (89.1%), bilateral (86.4%), and multilobar (89.1%) involvement, predominant distribution at peripheral (87.1%), posterior (46.3%), and lower (51.7%) lung areas were the other

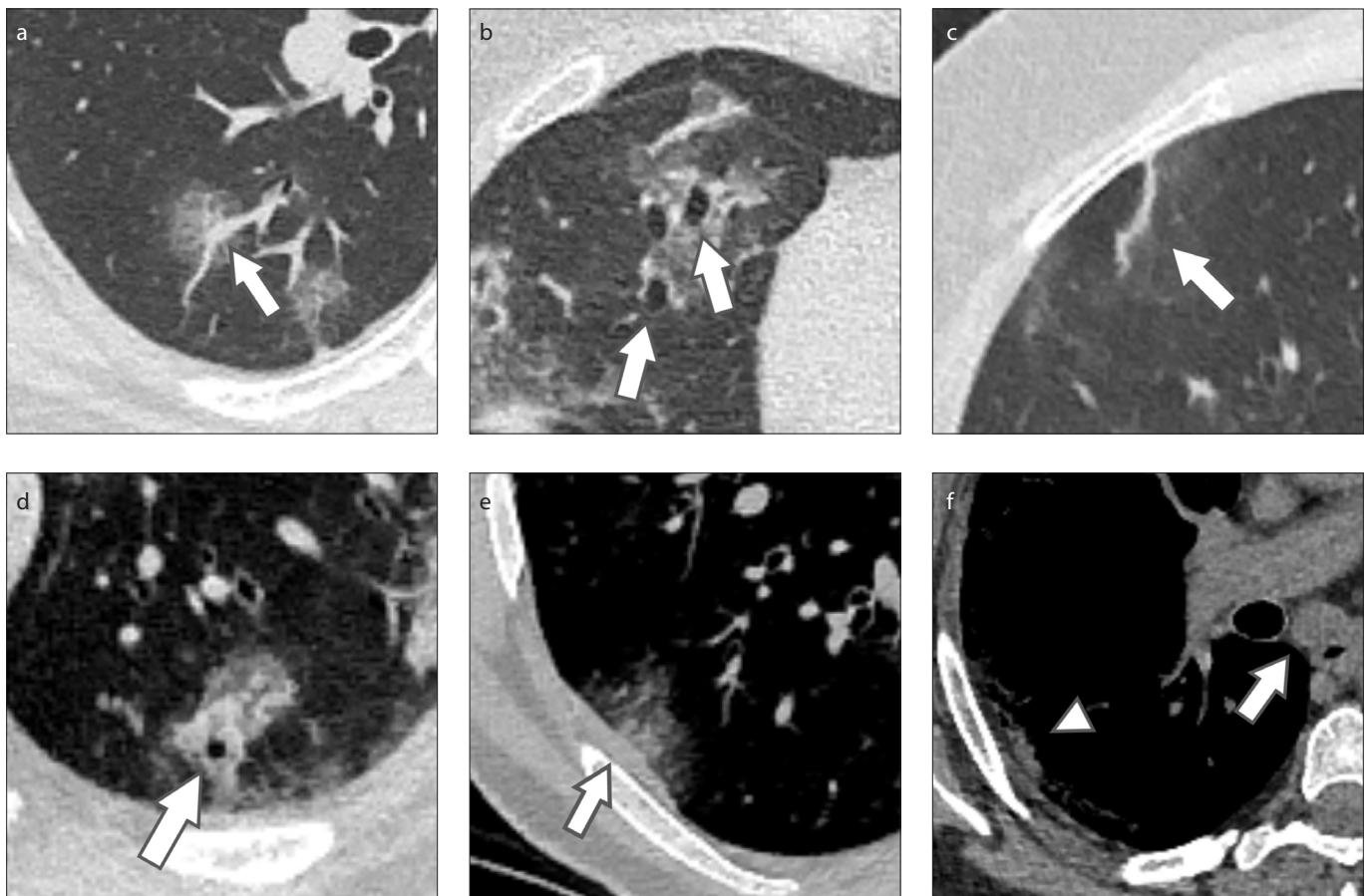


Figure 4. a-f. Other CT findings accompanying lung infiltration in COVID-19 pneumonia: (a), dilatation of pulmonary vessel within the GGO lesion consistent with “vascular enlargement” (arrow); (b), GGO with bronchial dilatation (bronchiectasis) (arrows); (c), a thin curvilinear opacity parallel to the pleura “subpleural line” (arrow); (d), consolidation with air-bubble sign (arrow); (e), pleural thickening (arrow) adjacent to the infiltration; and (f), subcarinal LAP (arrow) and parenchymal infiltration (arrowhead).

CT findings observed with high incidences. These features have been demonstrated as typical CT findings in several recent studies regarding COVID-19 pneumonia (7, 9, 13–16). Consistent with our study, Song et al. (16) reported pure GGO infiltration, involvement of multiple lobes, particularly the lower lobes with a peripheral or posterior distribution to be the main CT findings seen in the majority of patients. They revealed that the time period between the onset of symptoms and the CT scan was decisive on the density of lung lesions and there were more consolidated lung lesions in patients with 5 or more days from symptom onset to CT scan. There are other studies regarding the temporal course of CT findings (17–20). Pan et al. (20) reported GGO as the early stage finding (0–4 days after onset of the initial symptom), and bilateral, multilobar distribution with diffuse GGO, crazy paving pattern and consolidation as progressive stage CT findings (5–8 days after onset of the initial symptom). In our study, findings

indicating progression, such as GGO with consolidation (32.7%), crazy paving pattern (21.8%), reverse halo sign (15%), and pure consolidation (15%), were less common than pure GGO. However, two or more lobes were affected in 131 cases (89.1%) and of them, 54 (70.9%) had diffuse infiltration involving all of the lung lobes. We included CT images taken within a short time after hospitalization. But this is not an indication for early disease, as the time between symptom onset and hospitalization varies patient to patient. Imaging findings suggest that our study group consisted of patients predominantly at the early and progressive stages of the disease. However, this observation needs to be confirmed with clinical data and patient history. As an additional finding, we observed a slight tendency to right lower lobe involvement. Of 147 patients, 129 (87.8%) had right lower lobe infiltration and 7 had infiltration limited only to the right lower lobe. This might be related to the anatomical structure of

the airways. Short and straight course of the right bronchus might be the reason for this tendency (17).

Solid nodules with halo sign, air-bronchogram, air-bubble sign, subpleural line, parenchymal distortion, vascular enlargement, bronchiectasis, pleural thickening were the other CT features observed in our study at rates not to be underestimated. Among these, vascular enlargement was the most frequent finding and was present in 50 patients (34%). Ye et al. (9) emphasized that it was a common finding in their series and might be attributed to the damage and swelling of the capillary wall caused by pro-inflammatory factors. Subpleural line, described as a thin curvilinear opacity parallel to the pleural surface with 1–3 mm thickness, was another finding that might be related to pulmonary edema or fibrosis. Wu et al. (15) and Li et al. (21) both reported around 20% of patients, similar to our study (27.9%). Air-bubble sign was observed in 15 patients (10.2%). Air-bubbles cannot be seen

easily on the source images, and this may be the reason for this relatively low rate. However, creating minimum intensity projection (MinIP) images with a slab thickness of 4–5 mm is a way to make them noticeable (22). We rarely observed extraparenchymal findings such as mediastinal lymphadenopathy and pleural effusion, which show higher incidences among severe and critical patients (21). Other findings indicating severity, such as pneumothorax and pericardial effusion were not detected in our patient group.

Even though most of the COVID-19 patients share CT findings defined as typical, these findings are known to be nonspecific and can be seen in other infectious diseases. Li et al. (23) in their review article, focused on imaging characteristics of COVID-19 pneumonia and also made a comparison between COVID-19 and other diseases that have similar CT findings. Viral pneumonia (influenza pneumonia, respiratory syncytial virus pneumonia, rhinovirus pneumonia, adenovirus pneumonia), non-viral infectious pneumonia such as mycoplasma pneumonia, non-infectious pneumonia (hypersensitivity pneumonia, pulmonary alveolar proteinosis, interstitial pneumonia) should be considered in the differential diagnosis. CT findings such as bilateral reticulonodular opacities, tree-in-bud pattern, and cavitation that would suggest these alternative diagnoses were not present in our study group. However, overlapping of imaging features should not be underestimated and imaging findings should be supported with clinical findings. When we reviewed final radiologic reports of patients in our study, we realized that 131 of 147 CT examinations were reported as highly suspicious and/or consistent with COVID-19 pneumonia. However, the remaining 16 CT examinations were reported as low probability based on less common CT findings such as unilateral and unifocal involvement, multiple acinar nodules distributed along bronchovascular bundles, and others. It should be also reminded that COVID-19, severe acute respiratory syndrome (SARS), and Middle East respiratory syndrome (MERS), are caused by infectious agents which are members of coronaviridae family. Given the fact that viruses in the same viral family share a similar pathogenesis, imaging features are expected to be similar as well. Supporting this expectation, the most common CT findings in patients with MERS infection are predominantly subpleural and basilar infiltration, with more extensive GGO than consolidation

(24). At presentation, CT of SARS patients shows unilateral or bilateral GGO or consolidation, and in hospitalized patients, the abnormalities tend to progress to bilateral air-space consolidation (25). A comprehensive list of differential diagnoses including all these infectious and non-infectious diseases increases the responsibility of the radiologist. However, diagnosis, treatment, and follow-up of COVID-19 pneumonia is a teamwork in which, departments of emergency, microbiology, radiology, chest and infectious disease take part (26).

This study had two limitations. First, in our setting we did not have enough information about the clinical history of patients, e.g., the duration of the symptoms. Second, we did not include follow-up CT images of the patients. Therefore, the relationship between CT findings and the course of the disease could not be evaluated and it was not possible to make a classification based on the stage of the disease.

In conclusion, we demonstrated a diverse group of CT findings that can be seen in COVID-19 pneumonia. Multifocal and bilateral GGO infiltration, predominantly distributed in peripheral, posterior, and lower lung areas was the most common infiltration pattern. Findings compatible with non-viral infectious pneumonia, such as tree-in-bud pattern and cavitation, were not detected. Given the complementary role of chest CT in the early diagnosis, radiologists should be familiar with the CT findings suggestive of COVID-19 pneumonia.

Conflict of interest disclosure

The authors declared no conflicts of interest.

References

- Huang C, Wang Y, Li X, et al. Clinical features of patients infected with 2019 novel coronavirus in Wuhan, China. *Lancet* 2020; 395:497–506. [\[Crossref\]](#)
- World Health Organization (2020) Coronavirus disease 2019 (COVID-19) situation report–51. World Health Organization, Geneva. Available at: https://www.who.int/docs/default-source/coronaviruse/situation-reports/20200311-sitrep-51-covid-19.pdf?sfvrsn=1ba62e57_10.
- Turkish Government, Ministry of Health (2020). Available at: <https://covid19.saglik.gov.tr/>.
- Riou J, Althaus CL. Pattern of early human-to-human transmission of Wuhan 2019 novel coronavirus (2019-nCoV), December 2019 to January 2020. *Euro Surveill* 2020; 25:2000058. [\[Crossref\]](#)
- Kim H, Hong H, Yoon SH. Diagnostic performance of CT and reverse transcriptase-polymerase chain reaction for coronavirus disease 2019: A meta-analysis. *Radiology* 2020; 201343. [\[Crossref\]](#)

- Ai T, Yang Z, Hou H, et al. Correlation of chest CT and RT-PCR testing in coronavirus disease 2019 (COVID-19) in China: A report of 1014 cases. *Radiology* 2020; 200642. [\[Crossref\]](#)
- Fang Y, Zhang H, Xie J, et al. Sensitivity of chest CT for COVID-19: comparison to RT-PCR. *Radiology* 2020; 200432. [\[Crossref\]](#)
- Dai WC, Zhang HW, Yu J, et al. CT imaging and differential diagnosis of COVID-19. *Can Assoc Radiol J* 2020; 71:195–200. [\[Crossref\]](#)
- Ye Z, Zhang Y, Wang Y, Huang Z, Song B. Chest CT manifestations of new coronavirus disease 2019 (COVID-19): a pictorial review. *Eur Radiol* 2020 Mar 19. [Epub ahead of print] [\[Crossref\]](#)
- Hansell DM, Bankier AA, MacMahon H, McLoud TC, Müller NL, Remy J. Fleischner Society: glossary of terms for thoracic imaging. *Radiology* 2008; 246:697–722. [\[Crossref\]](#)
- Long C, Xu H, Shen Q, et al. Diagnosis of the coronavirus disease (COVID-19): rRT-PCR or CT? *Eur J Radiol* 2020; 126:108961. [\[Crossref\]](#)
- Bernheim A, Mei X, Huang M, et al. Chest CT findings in coronavirus disease-19 (COVID-19): relationship to duration of infection. *Radiology* 2020; 200463. [\[Crossref\]](#)
- Yoon SH, Lee KH, Kim JY, et al. Chest radiographic and CT findings of the 2019 novel coronavirus disease (COVID-19): analysis of nine patients treated in Korea. *Korean J Radiol* 2020; 21:494–500. [\[Crossref\]](#)
- Salehi S, Abedi A, Balakrishnan S, Gholamrezanezhad A. Coronavirus disease 2019 (COVID-19): a systematic review of imaging findings in 919 patients. *AJR Am J Roentgenol* 2020 Mar 14; 1–7. [Epub ahead of print] [\[Crossref\]](#)
- Wu J, Wu X, Zeng W, et al. Chest CT findings in patients with coronavirus disease 2019 and its relationship with clinical features. *Invest Radiol* 2020; 55:257–261. [\[Crossref\]](#)
- Song F, Shi N, Shan F, et al. Emerging 2019 novel coronavirus (2019-nCoV) pneumonia. *Radiology* 2020; 295:210–217. [\[Crossref\]](#)
- Shi H, Han X, Jiang N, et al. Radiological findings from 81 patients with COVID-19 pneumonia in Wuhan, China: a descriptive study. *Lancet Infect Dis* 2020; 20:425–434. [\[Crossref\]](#)
- Li M, Lei P, Zeng B, et al. Coronavirus disease (COVID-19): spectrum of CT findings and temporal progression of the disease. *Acad Radiol* 2020; 27:603–608. [\[Crossref\]](#)
- Li X, Zeng W, Li X, et al. CT imaging changes of corona virus disease 2019 (COVID-19): a multi-center study in Southwest China. *J Transl Med* 2020; 18:154. [\[Crossref\]](#)
- Pan F, Ye T, Sun P, et al. Time course of lung changes on chest CT during recovery from 2019 novel coronavirus (COVID-19) pneumonia. *Radiology* 2020; 295:715–721. [\[Crossref\]](#)
- Li K, Wu J, Wu F, et al. The clinical and chest CT features associated with severe and critical COVID-19 pneumonia. *Invest Radiol* 2020; 55:327–331. [\[Crossref\]](#)
- Savaş R. MinIP technique may be helpful in diagnosing COVID-19. *Diagn Interv Radiol* Published online 20 May 2020. 10.5152 / dir.2020.20295 [Epub Ahead of Print]. [\[Crossref\]](#)
- Li B, Li X, Wang Y, et al. Diagnostic value and key features of computed tomography in coronavirus disease 2019. *Emerg Microbes Infect* 2020; 9:787–793. [\[Crossref\]](#)

24. Aylan AM, Ahyad RA, Jamjoom LG, Alharthy A, Madani TA. Middle East respiratory syndrome coronavirus (MERS-CoV) infection: chest CT findings. *AJR Am J Roentgenol* 2014; 203:782–787. [\[Crossref\]](#)
25. Müller NL, Ooi GC, Khong PL, Nicolaou S. Severe acute respiratory syndrome: radiographic and CT findings. *AJR Am J Roentgenol* 2003; 181:3–8. [\[Crossref\]](#)
26. Çinkooğlu A, Bayraktaroglu S, Savas R. Lung changes on chest CT during 2019 novel coronavirus (COVID-19) pneumonia. *Eur J Breast Health* 2020; 16:89–90. [\[Crossref\]](#)